

Towards Rehearsal-Free Continual Relation Extraction: Capturing Within-Task Variance with Adaptive Prompting*

Bao-Ngoc Dao*, Quang Nguyen*, Luyen Ngo Dinh*, Minh Le*, Nam Le, Linh Ngo Van**

Hanoi University of Science and Technology, No. 1, Dai Co Viet road, Hanoi, Vietnam

Abstract

Memory-based approaches have shown strong performance in Continual Relation Extraction (CRE). However, storing examples from previous tasks increases memory usage and raises privacy concerns. Recently, prompt-based methods have emerged as a promising alternative, as they do not rely on storing past samples. Despite this progress, current prompt-based techniques face several core challenges in CRE, particularly in accurately identifying task identities and mitigating catastrophic forgetting. Existing prompt selection strategies often suffer from inaccuracies, lack robust mechanisms to prevent forgetting in shared parameters, and struggle to handle both cross-task and within-task variations. In this paper, we propose **WAVE++**, a novel approach inspired by the connection between prefix-tuning and mixture of experts. Specifically, we introduce task-specific prompt pools that enhance flexibility and adaptability across diverse tasks while avoiding boundary-spanning risks; this design more effectively captures variations within each task and across tasks. To further refine relation classification, we incorporate label descriptions that provide richer, more global context, enabling the model to better distinguish among different relations. We also propose a training-free mechanism to improve task prediction during inference. Moreover, we integrate a generative model to consolidate prior knowledge within the shared parameters, thereby removing the need for explicit data storage. Extensive experiments demonstrate that WAVE++ outperforms state-of-the-art prompt-based and rehearsal-based methods, offering a more robust solution for continual relation extraction. Our code is publicly available at <https://github.com/PiDinosauR2804/WAVE-CRE-PLUS-PLUS>.

Keywords: Continual Relation Extraction, Rehearsal-Free Learning, Prompting Techniques, Mixture of Experts, Label Descriptions, Ensemble Learning

1. Introduction

Continual Relation Extraction (CRE) involves training models to progressively extract relationships between entity pairs across a sequence of tasks (Wang et al., 2019; Zhao et al., 2022; Nguyen et al., 2023; Le et al., 2025a). As a specialized domain of continual learning, CRE’s primary goal is to mitigate *catastrophic forgetting* (McCloskey and Cohen, 1989; Nguyen et al., 2019), where model performance deteriorates as the

*A part of this work appears in Le et al. (2025a).

*Equal contribution

**Corresponding author

Email addresses: ngoc.db224884@sis.hust.edu.vn (Bao-Ngoc Dao), quang.nm144@gmail.com (Quang Nguyen), ngodinhluennht@gmail.com (Luyen Ngo Dinh), minh611002@gmail.com (Minh Le), namlh@soict.hust.edu.vn (Nam Le), linhnv@soict.hust.edu.vn (Linh Ngo Van)

number of tasks increases. To address this issue, most CRE methods *employ a memory buffer*, which stores samples for revisiting previous tasks and preserving previously learned knowledge (Han et al., 2020; Zhao et al., 2022). Approaches utilizing this strategy are commonly referred to as rehearsal-based methods.

While rehearsal-based methods have demonstrated notable success in mitigating catastrophic forgetting, they still exhibit significant limitations that call for more robust solutions. First, despite utilizing memory buffers, the representations of learned relations often degrade soon after training transitions to subsequent tasks (Caccia et al., 2021). Second, such methods violate a core principle of continual learning, as they necessitate ongoing access to datasets from earlier tasks. This reliance raises substantial concerns regarding *data privacy* and the considerable *storage demands* associated with large-scale memory buffers. Therefore, there is a pressing need to develop alternative approaches that minimize memory usage, thereby preserving the essence of continual learning while addressing privacy and scalability issues (Ke and Liu, 2022).

Recent advances in continual learning take inspiration from prompt-based techniques in natural language processing, leading to a new class of methods that leverage learnable parameters, known as *prompts*, to guide pre-trained models on downstream tasks without requiring access to past data (Wang et al., 2022b,a, 2024; Tran et al., 2024a). In contrast to traditional memory-replay methods, these approaches *do not rely on storing samples from previous tasks*; instead, they insert small sets of auxiliary parameters to steer the training process. These prompts are adaptable to specific tasks, enabling continual relation extraction without the necessity of data replay.

Despite these advantages, current prompt-based frameworks still exhibit several limitations. First, they do not fully alleviate catastrophic forgetting because many approaches *rely on shared prompts*, such as the Prompt Pool (Wang et al., 2022b), the General Prompt (G-Prompt) (Wang et al., 2022a), or a shared MLP classifier, thereby constraining their adaptability to varying task distributions. Second, the task-prediction mechanisms employed by these methods (Wang et al., 2022a, 2024) are *prone to misclassification errors*. Any mismatch between the prompts used during training and those employed at inference can degrade performance. Finally, prompt-based methods often *fail to address both cross-task and within-task variability*. For example, Wang et al. (2022b) introduce a common prompt pool, which can lead to multiple tasks sharing identical prompts and diminish cross-task diversity. This limitation is especially prominent in continual relation extraction, where instances from different relation classes may present almost identical contexts, illustrated by examples such as:

- "[X] is a student at [Z college]".
- "[X] supervises a student at [Z college]".

In alignment with these approaches, Le et al. (2024a) investigate the connection between *Prefix-tuning* (Li and Liang, 2021), a widely adopted prompt-based technique, and *Mixture of Experts (MoE)* models (Jacobs et al., 1991; Jordan and Jacobs, 1994). Their findings reveal that *self-attention can be interpreted as embedding multiple MoE models*, and that implementing prefix-tuning is akin to appending new *prefix experts* to these pre-trained MoE architectures, thereby enabling the fine-tuning of underlying representations.

Building on this insight, we propose **WAVE++** (Within-Task Variance Awareness for CRE), a prompt-based method designed to address the limitations outlined above. Rather than employing a single prompt pool across all tasks, WAVE++ assigns *a dedicated Prompt Pool for each task*, thereby improving plasticity in response to task distribution shifts and better capturing task-specific characteristics. Additionally, WAVE++ integrates *label descriptions* of relations to learn global, relation-specific contexts, ensuring that essential characteristics of each relation are preserved.

To mitigate catastrophic forgetting within the shared parameters, WAVE++ incorporates *generative models* that produce instructed latent data representations for replay. This strategy guards against representation drift

without requiring the storage of extensive raw data, offering a more efficient and comprehensive alternative to conventional replay-based methods. Further, although recent approaches often rely on a classifier head for task prediction (Wang et al., 2024; Le et al., 2025a), WAVE++ removes this dependency by *selecting the relevant prompt pool through a simple voting mechanism*. Experimental results demonstrate that WAVE++ achieves state-of-the-art performance, outperforming existing prompt-based and rehearsal-based baselines.

Contributions. Our main contributions can be summarized as follows:

- We identify key limitations in current prompt-based continual learning approaches, including ineffective prompt selection, inadequate mitigation of catastrophic forgetting in shared parameters, and suboptimal strategies for handling both cross-task and within-task variance.
- We highlight the underlying connections between mixture of experts models and prompt-based continual learning techniques. Specifically, we show that any prompt-based continual learning framework can be viewed as a specialized instance of MoE architectures.
- We propose **WAVE++**, which addresses the identified shortcomings by introducing task-specific prompt pools, leveraging relation label descriptions, employing a voting-based task prediction mechanism, and incorporating generative modeling of latent representations to enhance CRE performance.
- Through extensive experiments, we show that WAVE++ outperforms state-of-the-art prompt-based and rehearsal-based methods, validating both its effectiveness and versatility.

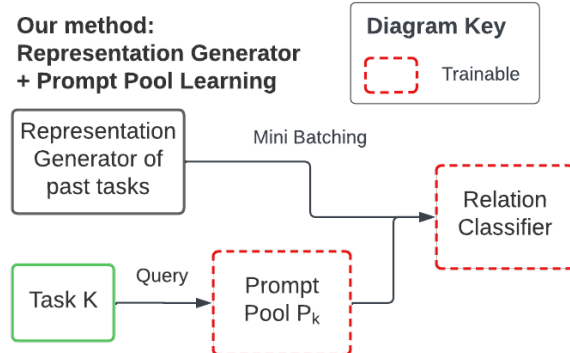


Figure 1: Overall framework of WAVE++. To mitigate forgetting across tasks, each k -th task is associated with its own prompt pool \mathcal{P}_k , rather than relying on a single, shared prompt pool as in L2P. In addition, we employ representation generators to synthesize information from previously learned tasks, thereby reinforcing the relation classifier’s capacity to retain accumulated knowledge.

2. Background and Related Work

In this section, we briefly describe the relevant background and discuss existing literature on continual relation extraction in Section 2.1. We then examine recent advancements in prompt-based approaches, followed by an overview of mixture of experts models in Section 2.2 and Section 2.3, respectively.

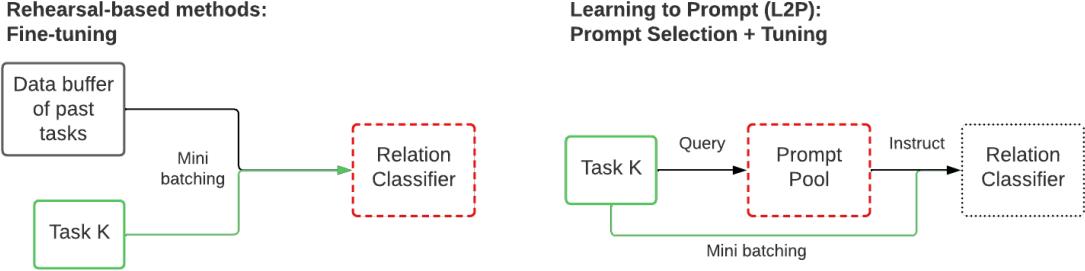


Figure 2: Comparison with rehearsal-based methods. Unlike approaches that rely on a rehearsal buffer, L2P employs a single backbone model and a Prompt Pool to store task-specific knowledge, thereby eliminating the need for explicit rehearsal to prevent forgetting. L2P further adapts to each instance by selecting and updating prompts from the pool on a per-instance basis.

2.1. Continual Relation Extraction

Relation extraction is a subfield of continual learning Hai et al. (2024); Phan et al. (2022); Van et al. (2022) and continual information extraction Le et al. (2024b); Dao et al. (2024); Tran et al. (2024b). It is a fundamental task in natural language processing (NLP) that aims at identifying semantic relationships between entities in unstructured text. By capturing how entities relate to one another, relation extraction facilitates deeper understanding of textual data and serves as a foundation for numerous downstream applications. *Continual relation extraction (CRE)* is a special branch of relation extraction that addresses the challenge of incrementally learning new relational patterns from incoming tasks while retaining the ability to recognize relations learned in previous tasks.

Formally, CRE involves learning sequentially from a series of tasks $\{\mathcal{T}_1, \dots, \mathcal{T}_k\}$, where \mathcal{T}_t denotes the t -th task. Similar to traditional supervised classification frameworks (Ji et al., 2020), each task \mathcal{T}_t is associated with a dataset $\mathcal{D}_t = \{(\mathbf{x}_i^t, y_i^t) \mid y_i^t \in \mathcal{R}_t\}_{i=1}^{\mathcal{N}_t}$ of \mathcal{N}_t input-label pairs and a distinct set of relations \mathcal{R}_t . Notably, these relation sets are mutually exclusive across tasks, such that $\mathcal{R}_i \cap \mathcal{R}_j = \emptyset$ for all $i \neq j$ and $i, j \in \{1, \dots, k\}$. Furthermore, once the model completes training on a given task t , it can no longer access the data from that task when learning subsequent tasks.

As training proceeds, the model must maintain its performance on all relations encountered so far, represented as $\mathcal{R}_t = \bigcup_{i=1}^t \mathcal{R}_i$. A primary challenge under these constraints is *catastrophic forgetting*, wherein performance on earlier tasks deteriorates as the model adapts to new tasks. (McCloskey and Cohen, 1989; Nguyen et al., 2019).

Many strategies have been explored to address this challenge. For instance, EA-EMR (Wang et al., 2019) introduces a technique that combines memory replay and embedding alignment to alleviate catastrophic forgetting. RP-CRE (Cui et al., 2021) employs a memory network to refine sample embeddings with relation prototypes. Similarly, CRE-DAS (Zhao et al., 2023) introduces memory-insensitive relation prototypes and memory augmentation to mitigate overfitting. CDec+ACA (Xia et al., 2023) proposes a classifier decomposition framework to address representation biases by promoting robust representation learning while preserving previously acquired knowledge. CREST (Le et al., 2024c) approaches the problem by training multiple objectives through sequential multi-task learning. However, *most existing approaches for CRE rely on the use of a memory buffer to store samples of previously encountered relations*, which raises critical concerns regarding both memory overhead and privacy (see Figure 2, left).

Recently, Kim et al. (2022) presented a theoretical framework that decomposes the continual learning

objective into more tractable components, offering a structured approach to mitigate catastrophic forgetting. Specifically, given a sample (\mathbf{x}, y) at test time with $y \in \mathcal{R}_t$, the model predicts the relation of this sample as \hat{y} . The probability of predicting the correct label, $\mathbb{P}(\hat{y} = y \mid \mathbf{x})$, is then factorized into two components: *within-task prediction* (WTP) and *task-identity inference* (TII), as follows:

$$\mathbb{P}(\hat{y} = y \mid \mathbf{x}) = \underbrace{\mathbb{P}(\hat{y} \in \mathcal{R}_t \mid \mathbf{x})}_{\text{Task-identity inference}} \times \underbrace{\mathbb{P}(\hat{y} = y \mid \hat{y} \in \mathcal{R}_t, \mathbf{x})}_{\text{Within-task prediction}}, \quad (1)$$

where the first term refers to the model’s ability to determine the appropriate task, and the second term represents the model’s ability to accurately predict the label within that task. It has been shown that improving these two components is both a *necessary* and *sufficient* condition to enhance overall continual learning performance. This framework provides a solid foundation for designing more effective rehearsal-free continual learning algorithms (Wang et al., 2024; Le et al., 2024a). In this work, we build on this theoretical framework by proposing methods to improve both TII and WTP (see Section 4 for details).

2.2. Prompt-based Approaches

Owing to robust generalization capabilities, recent studies have increasingly leveraged pre-trained models to mitigate catastrophic forgetting, demonstrating impressive performance gains (Wang et al., 2022b, 2023a,b; Zhou et al., 2024). In this work, we adopt a pre-trained BERT model (Devlin, 2018) as our base architecture, in line with previous research (Xia et al., 2023; Zhao et al., 2023). However, conventional fine-tuning of these models, which typically involves updating all parameters, poses substantial computational challenges.

To address these, *Parameter Efficient Fine-tuning* (PEFT) strategies have been proposed as an alternative paradigm (Houlsby et al., 2019; Hu et al., 2021; Lester et al., 2021; Li and Liang, 2021; Le et al., 2025b). PEFT focuses on designing fine-tuning methods that update only a small subset of parameters while leaving the rest of the model unchanged. By doing so, it significantly reduces the computational overhead associated with full fine-tuning. Among these techniques, *prompt-tuning* (Lester et al., 2021) and *prefix-tuning* (Li and Liang, 2021) have emerged as simple yet effective methods. Both approaches append learnable *prompt* tokens to the input—either at the input layer alone or also within intermediate representations—to serve as instructions for the pre-trained Transformer model to adapt to downstream tasks. Specifically, the Transformer architecture comprises multiple consecutive *multi-head self-attention* (MSA) layers (Vaswani, 2017), which are defined as follows:

Definition 2.1 (Multi-head Self-Attention Layer). Let $\mathbf{X}^Q = \mathbf{X}^K = \mathbf{X}^V = [\mathbf{x}_1, \dots, \mathbf{x}_N]^\top \in \mathbb{R}^{N \times d}$ be the input query, key, and value matrices, where N is the sequence length and d is the embedding dimension. The MSA layer output is given by:

$$\begin{aligned} \text{MSA}(\mathbf{X}^Q, \mathbf{X}^K, \mathbf{X}^V) &= \text{Concat}(\mathbf{h}_1, \dots, \mathbf{h}_m) W^O \in \mathbb{R}^{N \times d}, \\ \mathbf{h}_i &= \text{Attention}(\mathbf{X}^Q W_i^Q, \mathbf{X}^K W_i^K, \mathbf{X}^V W_i^V) \in \mathbb{R}^{N \times d_v}, \end{aligned} \quad (2)$$

where m is the number of attention heads, and $W_i^Q \in \mathbb{R}^{d \times d_k}$, $W_i^K \in \mathbb{R}^{d \times d_k}$, $W_i^V \in \mathbb{R}^{d \times d_v}$, $W^O \in \mathbb{R}^{md_v \times d}$ are the projection matrices. Typically $d_k = d_v = d/m$ so that the total output dimension remains d .

Building on the attention mechanism, prompt-tuning and prefix-tuning introduce learnable prompt parameters at the inputs of these MSA layers, enabling efficient fine-tuning of the pre-trained Transformer model.

Definition 2.2 (Prompt-tuning). Let $\mathbf{P} = [p_1, \dots, p_L]^\top \in \mathbb{R}^{L \times d}$ be the prompt parameters, where L denotes the prompt length. Prompt-tuning appends the same prompt parameters to the query, key, and value matrices:

$$f_{\text{prompt}}^{\text{Pro-T}}(\mathbf{P}, \mathbf{X}^Q, \mathbf{X}^K, \mathbf{X}^V) = \text{MSA} \left(\begin{bmatrix} \mathbf{P} \\ \mathbf{X}^Q \end{bmatrix}, \begin{bmatrix} \mathbf{P} \\ \mathbf{X}^K \end{bmatrix}, \begin{bmatrix} \mathbf{P} \\ \mathbf{X}^V \end{bmatrix} \right) \in \mathbb{R}^{(N+L) \times d}. \quad (3)$$

Definition 2.3 (Prefix-tuning). Let $\mathbf{P} = [\mathbf{P}^K; \mathbf{P}^V]$, where $\mathbf{P}^K = [p_1^K, \dots, p_L^K]^\top \in \mathbb{R}^{L \times d}$ and $\mathbf{P}^V = [p_1^V, \dots, p_L^V]^\top \in \mathbb{R}^{L \times d}$ are the prefix key and prefix value parameters, respectively. Prefix-tuning injects these parameters into the key and value matrices:

$$f_{\text{prompt}}^{\text{Pre-T}}(\mathbf{P}, \mathbf{X}^Q, \mathbf{X}^K, \mathbf{X}^V) = \text{MSA} \left(\mathbf{X}^Q, \begin{bmatrix} \mathbf{P}^K \\ \mathbf{X}^K \end{bmatrix}, \begin{bmatrix} \mathbf{P}^V \\ \mathbf{X}^V \end{bmatrix} \right) \in \mathbb{R}^{N \times d}. \quad (4)$$

Unlike prompt-tuning, prefix-tuning does not prepend prompts to the query matrix, thereby preserving the original input sequence dimension. In this study, we focus on prefix-tuning for prompt implementation. Note that only the prompt parameters \mathbf{P} are trained, while the parameters of the pre-trained Transformer backbone including W_i^Q , W_i^K , W_i^V , and W^O remain frozen throughout training.

Inspired by these prompting techniques, several recent methods have successfully incorporated them into continual learning, providing a flexible and robust strategy to mitigate catastrophic forgetting without the need to store historical data, such as L2P (Wang et al., 2022b), DualPrompt (Wang et al., 2022a), and HiDe-Prompt (Wang et al., 2024). A more detailed discussion of these methods is presented in Section 3.

2.3. Mixture of Experts

Mixture of Experts (MoE) is a classical ensemble learning framework that combines multiple models to achieve more expressive and accurate predictions (Jacobs et al., 1991; Jordan and Jacobs, 1994). Formally, an MoE model consists of N *expert networks*, denoted by $f_i : \mathbb{R}^d \rightarrow \mathbb{R}^{d_v}$ for $i = 1, \dots, N$. A *gating function*, $G : \mathbb{R}^d \rightarrow \mathbb{R}^N$, then dynamically determines the contribution of each expert for a given input $\mathbf{x} \in \mathbb{R}^d$. The gating function depends on a set of learned *score functions*, $s_i : \mathbb{R}^d \rightarrow \mathbb{R}$, associated with each expert, resulting in the following formulation:

$$\mathbf{y} = \sum_{j=1}^N G(\mathbf{x})_j \cdot f_j(\mathbf{x}) = \sum_{j=1}^N \frac{\exp(s_j(\mathbf{x}))}{\sum_{\ell=1}^N \exp(s_\ell(\mathbf{x}))} \cdot f_j(\mathbf{x}),$$

where $G(\mathbf{x}) = \text{softmax}(s_1(\mathbf{x}), \dots, s_N(\mathbf{x}))$. Building on this concept, Shazeer et al. (2017) proposed *Sparse Mixture of Experts* (SMoE) architecture to efficiently scale up large models. This is achieved by utilizing a sparse gating function TopK, which selects only the K experts with the highest scores $s_j(\mathbf{x})$ and assigns a weight of $-\infty$ to the remaining experts. Formally, the TopK function is defined as:

$$\text{TopK}(\mathbf{v}, K)_i = \begin{cases} \mathbf{v}_i, & \text{if } \mathbf{v}_i \text{ is in the } K \text{ largest elements of } \mathbf{v} \\ -\infty, & \text{otherwise.} \end{cases}$$

After the gating function selects the top K experts, these experts independently compute their outputs, which are then linearly combined via their normalized scores:

$$\mathbf{y} = \sum_{j=1}^N \text{softmax}(\text{TopK}(s(\mathbf{x}), K))_j \cdot f_j(\mathbf{x}),$$

where $s(\mathbf{x}) = (s_1(\mathbf{x}), \dots, s_N(\mathbf{x}))$. MoE has attracted considerable attention due to their flexibility and adaptability across various domains, including large language models (Du et al., 2022; Zhou et al., 2023; Li et al., 2024), computer vision (Riquelme et al., 2021), and multi-task learning (Ma et al., 2018).

3. From Mixture of Experts to Prompt-based Continual Learning

In this section, we discuss the relationship between mixture of experts and prompt-based techniques, and demonstrate how existing prompt-based continual learning methods can be interpreted within this framework. Specifically, recent work (Le et al., 2024a, 2025c) has shown that each output vector from each attention head in an MSA layer can be viewed as the output of an MoE model. This perspective implies that an MSA layer can be regarded as a special architecture in which *each attention head comprises multiple MoE models*. Furthermore, these studies suggest that prefix-tuning can be interpreted as *introducing new experts* to fine-tune these MoE models.

Specifically, let $\mathbf{X} = [\mathbf{x}_1^\top, \dots, \mathbf{x}_N^\top]^\top \in \mathbb{R}^{Nd}$ denote the concatenation of all input token embeddings. We define $E_j \in \mathbb{R}^{d \times Nd}$ as a standard basis selector such that $E_j \mathbf{X} = \mathbf{x}_j$, thereby extracting the j -th token from the input sequence. From Equation (2), the output of the l -th attention head is $\mathbf{h}_l = [\mathbf{h}_{l,1}, \dots, \mathbf{h}_{l,N}]^\top \in \mathbb{R}^{N \times d_v}$. Each output vector $\mathbf{h}_{l,i} \in \mathbb{R}^{d_v}$ can then be expressed as an MoE model:

$$\mathbf{h}_{l,i} = \sum_{j=1}^N \frac{\exp s_{i,j}(\mathbf{X})}{\sum_{k=1}^N \exp s_{i,k}(\mathbf{X})} \cdot f_j(\mathbf{X}), \quad (5)$$

where the expert $f_j : \mathbb{R}^d \rightarrow \mathbb{R}^{d_v}$, and the score function $s_{i,j} : \mathbb{R}^d \rightarrow \mathbb{R}$ are given by:

$$f_j(\mathbf{X}) = W_l^{V^\top} E_j \mathbf{X} = W_l^{V^\top} \mathbf{x}_j, \quad (6)$$

$$s_{i,j}(\mathbf{X}) = \frac{\mathbf{X}^\top E_i^\top W_l^Q W_l^{K^\top} E_j \mathbf{X}}{\sqrt{d_v}} = \frac{\mathbf{x}_i^\top W_l^Q W_l^{K^\top} \mathbf{x}_j}{\sqrt{d_v}}, \quad (7)$$

for $i, j = 1, \dots, N$. This structure is analogous to the *Multi-gate Mixture of Experts* framework (Ma et al., 2018), where multiple MoE models share a common set of experts but use distinct gating functions, as illustrated in Figure 3.

When the model is pre-trained, all weights W_l^Q , W_l^K , and W_l^V were previously learned and then, they are held fixed, so the parameters of the experts f_j and score functions $s_{i,j}$ remain frozen. Consequently, these pre-trained experts f_1, \dots, f_N can be regarded as a knowledge base. Prefix-tuning augments this knowledge base by introducing additional *prefix experts* encoded in prompt tokens. Specifically, the new experts and score functions are defined as follows:

$$f_{N+j'}(\mathbf{X}) = W_l^{V^\top} \mathbf{p}_{j'}, \quad (8)$$

$$s_{i,N+j'}(\mathbf{X}) = \frac{\mathbf{X}^\top E_i^\top W_l^Q W_l^{K^\top} \mathbf{p}_{j'}}{\sqrt{d_v}} = \frac{\mathbf{x}_i^\top W_l^Q W_l^{K^\top} \mathbf{p}_{j'}}{\sqrt{d_v}}, \quad (9)$$

for $j' = 1, \dots, L$ and $i = 1, \dots, N$. From Equation (4), the output of the l -th attention head modified by prefix-tuning can be written as:

$$\tilde{\mathbf{h}}_l = \text{Attention} \left(\mathbf{X}^Q W_l^Q, \begin{bmatrix} \mathbf{P}^K \\ \mathbf{X}^K \end{bmatrix} W_l^K, \begin{bmatrix} \mathbf{P}^V \\ \mathbf{X}^V \end{bmatrix} W_l^V \right) = [\tilde{\mathbf{h}}_{l,1}, \dots, \tilde{\mathbf{h}}_{l,N}]^\top \in \mathbb{R}^{N \times d_v}, \quad (10)$$

where each output vector $\tilde{\mathbf{h}}_{l,i} \in \mathbb{R}^{d_v}$ can be demonstrated as an MoE model:

$$\tilde{\mathbf{h}}_{l,i} = \underbrace{\sum_{j=1}^N \frac{\exp(s_{i,j}(\mathbf{X}))}{\sum_{k=1}^{N+L} \exp(s_{i,k}(\mathbf{X}))} f_j(\mathbf{X})}_{\text{pre-trained experts}} + \underbrace{\sum_{j'=1}^L \frac{\exp(s_{i,N+j'}(\mathbf{X}))}{\sum_{k=1}^{N+L} \exp(s_{i,k}(\mathbf{X}))} f_{N+j'}(\mathbf{X})}_{\text{new prefix experts}}, \quad (11)$$

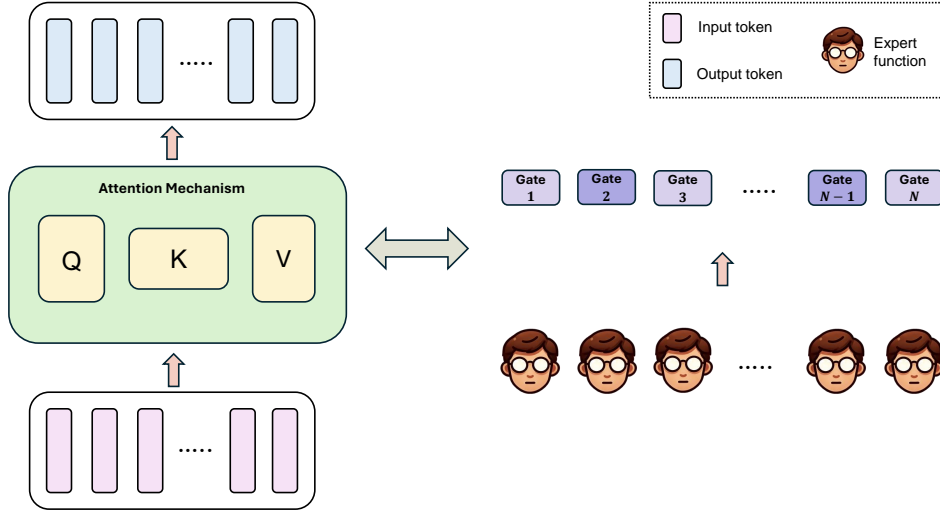


Figure 3: Illustration of the connection between attention and mixture of experts. Each attention head can be viewed as consisting of multiple MoE modules that share a common set of experts but employ different gating functions. This design closely parallels the multi-gate MoE architecture.

for $i = 1, \dots, N$. Hence, prefix-tuning can be interpreted as adding new experts f_{N+1}, \dots, f_{N+L} to the original pre-trained experts f_1, \dots, f_N . These additional experts collaborate with the original ones to adapt the model for downstream tasks, alleviating the need to retrain all parameters of the model. This perspective offers a new way to analyze and explore existing prompt-based continual learning methods. Here we take L2P (Wang et al., 2022b) as a concrete example.

L2P introduces the concept of a *Prompt Pool*, consisting of multiple prompts that guide the pre-trained model to adapt to all tasks. Specifically, let the pool of M prompts be

$$\mathcal{P} = \{(\mathbf{k}_1, \mathbf{P}_1), \dots, (\mathbf{k}_M, \mathbf{P}_M)\}, \quad (12)$$

where each prompt $\mathbf{P}_i \in \mathbb{R}^{L \times d}$ is associated with a learnable key $\mathbf{k}_i \in \mathbb{R}^d$ for $i = 1, \dots, M$. Given an input instance \mathbf{x} , we first compute a query vector $q(\mathbf{x}) \in \mathbb{R}^d$ using the pre-trained Transformer model. We then employ a query-key matching function $\gamma : \mathbb{R}^d \times \mathbb{R}^d \rightarrow \mathbb{R}$ (e.g., cosine similarity) to select top- K most relevant prompts by solving the following objective:

$$\mathbf{K}_{\mathbf{x}} = \underset{S \subseteq \{1, \dots, M\}: |S|=K}{\operatorname{argmin}} \sum_{s \in S} \gamma(q(\mathbf{x}), \mathbf{k}_s), \quad (13)$$

where $\mathbf{K}_{\mathbf{x}}$ is the subset of indices for the top- K keys most relevant to \mathbf{x} . The corresponding prompts are then prepended to \mathbf{x} to form the prompted input \mathbf{x}_p , which is finally fed back into the Transformer model to generate the final prediction. By serving as a repository of task-specific knowledge, the prompt pool removes the need for a rehearsal buffer to prevent catastrophic forgetting (see Figure 2, right).

The prompt pool can be viewed as a collection of $M \cdot L$ experts f_{N+1}, \dots, f_{N+ML} . Each prompt \mathbf{P}_i implicitly encodes a group of L experts, $f_{N+(i-1)L+1}, \dots, f_{N+iL}$ for $i = 1, \dots, M$. Consequently, selecting K prompts from the pool is analogous to selecting $K \times L$ experts. Each expert is assigned based on the query

feature $q(\mathbf{x})$, which captures contextual information. However, because each prompt P_i is associated with a single prompt key k_i , *all L experts within a given prompt is tied to a single prompt key k_i* , potentially limiting the model’s expressiveness. Moreover, employing a single prompt pool for all tasks can lead to issues like forgetting or noisy knowledge, as *instances from different tasks may share certain experts*, thereby reducing cross-task variability.

DualPrompt (Wang et al., 2022a) enhances L2P by using two complementary prompts: a general prompt (G-Prompt) and a task-specific expert prompt (E-Prompt) per task. When a new task arrives, only the G-Prompt and the newly introduced E-Prompt for that task are updated during training, while previously encountered E-Prompts remain fixed. The set of E-Prompts serves as an expanding pool of task-specific knowledge, similar to the L2P prompt pool, but with the key difference of growing incrementally with each new task. DualPrompt retains L2P’s prompt selection mechanism for E-Prompts. In contrast, G-Prompt is shared between all tasks, which requires no prompt selection. We posit that the G-Prompt aims to augment the set of pre-trained experts f_1, \dots, f_N by introducing additional experts capturing generalizable knowledge. However, in contrast to pre-trained experts, these newly learned experts in the G-Prompt are continually updated across tasks, thereby making them susceptible to forgetting.

HiDe-Prompt (Wang et al., 2024), by comparison, uses only task-specific E-Prompts. For prompt selection, it leverages an auxiliary MLP head trained with cross-entropy loss to select the appropriate prompt, *treating each task as a separate class*. This class-based approach may be suboptimal because classes are defined by task order rather than semantic distinctions. Moreover, *restricting each task to a single prompt may be insufficient to capture its full complexity*, given the limited expressiveness of prefix-tuning (Petrov et al., 2023). Specifically, prefix experts represent offset vectors encoded by prompt tokens, rather than the linear functions used by pre-trained experts, as indicated in Equation (6) and Equation (8). This simplicity limits their capacity to accommodate the full range of variations within each task. We address these concerns in Section 4.

4. Proposed Method

In this section, we present our proposed method WAVE++ in detail. First, in Section 4.1, we examine the relationship between the mixture of experts and prefix-tuning to develop task-specific prompt pools that capture the inherent variations within individual tasks. Next, in Section 4.2, we introduce label descriptions combined with a contrastive loss to enhance the robustness of each prompt pool by encapsulating the essential characteristics of task relations. These two components collectively improve within-task performance and contribute to enhanced continual learning, as demonstrated in Equation (1). Lastly, we employ cascade voting for task prediction (Section 4.3) and generative models to mitigate classification bias toward previously learned tasks in the relation classifier (Section 4.4). An overview of our complete framework is provided in Figure 1.

4.1. Task-specific Prompt Pool

As discussed in Section 3, recent advances in continual learning, such as HiDe-Prompt (Wang et al., 2024), typically employ a dedicated prompt for each task. Although these task-specific prompts help mitigate catastrophic forgetting by leveraging specialized features, relying on a single prompt for all instances within a task can be overly restrictive. In particular, these prefix experts are simply constant functions, rendering them invariant to input variation. We posit that this limited expressiveness hinders the model from capturing the full complexity and variability inherent in each task.

A straightforward strategy to enhance the expressiveness of prefix experts is to replace the constant function with a more complex one, such as a linear function. However, a key advantage of the original

design lies in its simplicity and cost-effectiveness. A naive implementation of a more expressive prefix would therefore risk significantly increasing computational overhead, thus negating the practical benefits of the original approach. An alternative approach, exemplified by L2P (Wang et al., 2022b), involves maintaining a prompt pool from which prompts are selected based on the query features $q(\mathbf{x})$. In this way, the set of experts is adaptively chosen according to the input, yielding a configuration similar to an SMoE architecture. This design achieves greater expressiveness while retaining efficiency.

Despite these advantages, repeatedly using the same prompts across different tasks increases the likelihood of overlap between them. Such overlap introduces the risk of overwriting task-specific knowledge, potentially erasing important information tailored to each task. Consequently, prompts may fail to capture the essential knowledge or requirements of individual tasks, leading to suboptimal within-task performance. To address this challenge, we propose constructing *a prompt pool for each task*, ensuring that each task maintains its distinct prompt allocation, thus reducing the risk of undesired overlap.

Specifically, for the t -th task, following the formulation presented in Equation (12), we introduce a prompt pool \mathcal{P}_t consisting of M prompts, defined as follows:

$$\mathcal{P}_t = \left\{ (\mathbf{k}_1^{(t)}, \mathbf{P}_1^{(t)}), \dots, (\mathbf{k}_M^{(t)}, \mathbf{P}_M^{(t)}) \right\}. \quad (14)$$

Each prompt $\mathbf{P}_i^{(t)} \in \mathbb{R}^{L \times d}$ is associated with a learnable key $\mathbf{k}_i^{(t)} \in \mathbb{R}^d$. For prompt selection, we employ the same query-key mechanism as in L2P. We use cosine similarity for the scoring function $\gamma : \mathbb{R}^d \times \mathbb{R}^d \rightarrow \mathbb{R}$ to measure the distance between the query feature $q(\mathbf{x})$, encoded using a pre-trained BERT model, and the prompt keys. The top- K most relevant prompts in the prompt pool \mathcal{P}_t are selected by optimizing the following objective:

$$\mathbf{K}_x = \underset{S \subseteq \{1, \dots, M\}: |S|=K}{\operatorname{argmin}} \sum_{s \in S} \gamma(q(\mathbf{x}), \mathbf{k}_s^{(t)}), \quad (15)$$

where \mathbf{K}_x is the set of prompt selected for the instance \mathbf{x} . Additionally, we introduce a *prompt pool loss*, as in L2P, to facilitate prompt selection:

$$\mathcal{L}_{pp} = \sum_{s \in \mathbf{K}_x} \gamma(q(\mathbf{x}), \mathbf{k}_s^{(t)}). \quad (16)$$

However, incorporating a prompt pool for each task may significantly increase computational costs, as each task uses multiple prompts. To address this, we configure each prompt with a single prefix expert by setting $L = 1$, thereby reducing the memory cost. This approach mirrors other methods that employ a single prompt per task but with greater length. Additionally, using longer prompts would introduce multiple experts per prompt, each sharing a common prompt key $\mathbf{k}_i^{(t)}$. Our configuration reduces memory overhead while enhancing flexibility in expert selection during both training and testing. It allows each expert to specialize based on the input, offering a more adaptable assignment compared to methods that rely on multiple experts per prompt.

Our architecture enables the assignment of distinct sets of experts to specific regions of the input data, guided by the contextual query feature $q(\mathbf{x})$. This design allows each prompt in the pool to focus on the relevant information and patterns crucial for optimal performance in different regions of the input domain. As a result, the model effectively captures within-task variations. Moreover, by utilizing a task-specific prompt pool, we minimize the need for parameter sharing, thereby maximizing cross-task variance and improving overall task performance.

Comparison to Sparse Mixture of Experts. We demonstrate that our proposed task-specific prompt pool, or more generally, the prompt pool, shares several similarities with the SMoE architecture discussed in Section 2.3. Specifically, from Equation (14), by setting $L = 1$, where each prompt encodes only a single prefix expert, the experts encoded in the prompt pool \mathcal{P}_t are denoted as $f_{N+1}^{(t)}, \dots, f_{N+M}^{(t)}$. Unlike the pre-trained experts f_1, \dots, f_N in the pre-trained BERT, which are selected by default, we employ sparse selection exclusively for these newly introduced prefix experts. As illustrated in Equation (11), each head in the MSA layer, when applying prefix-tuning, encompasses N MoE models $\tilde{h}_{l,1}, \dots, \tilde{h}_{l,N}$. A naive approach would involve applying the TopK function to each of these N models individually, requiring the computation of all $N \times M$ score functions $s_{i,N+j'}(\mathbf{X})$ for $i = 1, \dots, N$ and $j' = 1, \dots, M$. This can lead to a distinct set of prefix experts selected for each model. In contrast, our strategy utilizes the same set of K new experts across all N MoE models using auxiliary score functions defined as:

$$\tilde{s}_{i,N+j'}(\mathbf{X}) = \gamma(q(\mathbf{x}), \mathbf{k}_{j'}^{(t)}), \quad (17)$$

where $i = 1, \dots, N$ and $j' = 1, \dots, M$. This strategy requires the computation of only M score functions, as $\tilde{s}_{i,N+j'}(\mathbf{X})$ depends solely on $\mathbf{k}_{j'}^{(t)}$, thereby enabling efficient and effective selection of K experts from the prompt pool. Although the calculation of $q(\mathbf{x})$ might seem like an additional expense, this value is already computed for the task predictor in Section 4.3 during both the training and testing phases. As a result, the computation of $q(\mathbf{x})$ can be reused without incurring any extra cost in the prompt selection process.

4.2. Enhancing Training with Label Descriptions

Let the embeddings of the input sequence \mathbf{x} be denoted as \mathbf{x}_e , and the input embedding after incorporating prompts via prefix-tuning as \mathbf{x}_p . The model’s output is then given by $g_\phi(f_\theta(\mathbf{x}_p))$, where f_θ represents the pre-trained transformer encoder and g_ϕ is the final relation classifier, parameterized by ϕ .

In our framework, each task is associated with a distinct prompt pool. At test time, determining which prompt pool to apply for a given sample can be prone to errors, potentially leading to the use of an inappropriate prompt pool. Such misalignment may result in suboptimal or incorrect predictions. To mitigate this risk, we seek to improve the global generalization capacity of each prompt pool, anticipating that it may encounter samples from tasks it was not originally designed for.

To achieve this, we propose incorporating *label-description representations into the training objective* for each prompt pool as an auxiliary resource. These representations capture the core attributes of each relation, providing global information that helps reduce overfitting and improve model robustness. Previous studies have demonstrated that label descriptions can significantly benefit CRE tasks by providing additional context on relation types (Yang et al., 2020; Liu et al., 2022; Borchert et al., 2024; Luo et al., 2024; Thanh et al., 2025). Notably, they offer a consistent, class-specific global perspective, enabling the model to focus on essential relational characteristics and avoid spurious features.

Specifically, we leverage the detailed definitions provided for each label, typically available in benchmarking datasets, which we refer to as *Raw descriptions*. However, relying solely on these raw descriptions may not offer sufficient diversity and richness, leading to potential noise and instability, which could harm model performance. To address these limitations, we follow prior work (Thanh et al., 2025) and employ Gemini 1.5 (Team et al., 2023, 2024) to generate D diverse, detailed, and illustrative descriptions for each relation. For each label, the raw description is fed into the large language model (LLM), serving as an expert-in-the-loop to guide the model. A depiction of our prompt template is shown in Table 1.

The generated descriptions are then processed by a pre-trained BERT model to obtain their corresponding description representations. For task t , each relation $r \in \mathcal{R}_t$ is associated with a set of label description representations $Des_r = \{\mathbf{d}_{r,i} \in \mathbb{R}^d \mid i = 1, \dots, D\}$. Given an input \mathbf{x} , our objective is to train prompts that

Prompt for generate label description

You are a professional data scientist, working in a relation extraction project.

Given a relation and its description, you are asked to write a more detailed description of the relation and provide 3 sentence examples of the relation.

The relation is: place served by transport hub

The description is: territorial entity or entities served by this transport hub (airport, train station, etc.)

Please generate 2 diverse samples of (relation description, examples).

Your response:

Output:

This relation identifies the geographic areas or communities that are directly connected to and supported by a specific transport hub, such as an airport, train station, or bus terminal, emphasizing the role of the hub in providing access to transportation services for these areas.

Examples:

- Heathrow Airport serves the Greater London area, providing access to travelers from London and surrounding towns.
- Union Station in Washington, D.C. serves the metropolitan area, facilitating travel for residents and visitors in Maryland and Virginia.
- Los Angeles International Airport (LAX) serves not only Los Angeles but also the wider Southern California region, including cities like Santa Monica and Long Beach.

This relation captures the locations or regions that benefit from the operational capabilities of a transport hub, highlighting its significance in regional connectivity and economic activity.

Examples:

- Chicago O'Hare International Airport serves the entire Chicago metropolitan area, enhancing accessibility for surrounding suburbs.
- Penn Station in New York City is a critical transport hub that serves travelers from New Jersey, New York, and Connecticut.
- Dallas/Fort Worth International Airport serves the Dallas and Fort Worth areas, acting as a key transit point for the entire North Texas region.

Table 1: Example generated label descriptions

guide the input to the correct relation y . We aim to pull $f_\theta(\mathbf{x}_p)$ closer to the label description representation of the correct relation while pushing it away from the representations of other labels. To achieve this, we introduce a *contrastive loss* that enforces clearer separation between the target label and irrelevant labels:

$$\mathcal{L}_{cl} = -\log \frac{\sum_{\mathbf{d}_y \in Des_y} \exp(f_\theta(\mathbf{x}_p) \cdot \mathbf{d}_y)}{\sum_{r \in \hat{\mathcal{R}}_t} \sum_{\mathbf{d}_r \in Des_r} \exp(f_\theta(\mathbf{x}_p) \cdot \mathbf{d}_r)}, \quad (18)$$

where Des_y is the set of description representations for the true label y . This loss ensures that the representation of the input sample is strongly associated with its corresponding label while reducing its association with incorrect labels, thereby enhancing the model's discriminative power. Consequently, incorporating label descriptions improves the stability and reliability of learned representations, ensuring better performance even when faced with previously unseen or misclassified samples.

Optimization Objective. For each new task \mathcal{T}_t , a corresponding prompt pool \mathcal{P}_t is created. During each training step, as described in the aforementioned strategy, K prompts are selected, and the associated prompted embedding feature, denoted as \mathbf{x}_p , is fed into the pre-trained transformer encoder f_θ and the final classifier

Algorithm 1 Cascade Voting Mechanism

Input: Voting results $\mathcal{V}^0(\mathbf{x})$ and $\mathcal{V}^1(\mathbf{x})$ of prompt pool \mathcal{P}_0 and \mathcal{P}_1 , Maximum allowed experts m , Confidence scores $\{\text{Score}_t^i(\mathbf{x}) \mid 2 \leq i \leq k-1, i \leq t \leq k\}$

Output: Voting result $\mathcal{V}(\mathbf{x})$

```
1: if  $\mathcal{V}^0(\mathbf{x}) = \mathcal{V}^1(\mathbf{x})$  then
2:   return  $\mathcal{V}^0(\mathbf{x})$ 
3: end if
4:  $start = 0$ 
5:  $end = \min(\min(\mathcal{V}^0(\mathbf{x}), \mathcal{V}^1(\mathbf{x})), m)$ 
6:  $result = \text{dict}()$ 
7: for  $i \leftarrow start$  to  $end$  do
8:   Determine  $\mathcal{V}^i(\mathbf{x})$  via Equation (23)
9:    $result[\mathcal{V}^i(\mathbf{x})] += 1$ 
10: end for
11: return  $\arg \max_c result[c]$ 
```

g_ϕ . The overall objective can be expressed as follows:

$$\min_{\mathcal{P}_t, \phi} \mathcal{L}(g_\phi(f_\theta(\mathbf{x}_p)), y) + \alpha \mathcal{L}_{pp} + \beta \mathcal{L}_{cl}, \quad (19)$$

where α and β are hyperparameters. The first term in Equation (19) represents the classification loss. Importantly, only the prompt parameters in the current task’s prompt pool \mathcal{P}_t and the final classifier g_ϕ are updated during task t training. The pre-trained BERT model and all previous prompt pools $\mathcal{P}_1, \dots, \mathcal{P}_{t-1}$ remain frozen. By incorporating task-specific prompt pools and label descriptions, we propose a comprehensive training framework that enhances the model’s ability to accurately predict relations within each task. This approach *improves within-task prediction performance*, thereby contributing to better continual learning performance as shown in Equation (1). In the following section, we introduce our strategy to further enhance task-identity inference performance.

4.3. Cascade Voting for Task Prediction

During training, the model is provided with a dataset corresponding to a specific task and optimizes the associated task-specific prompt pool. However, during inference, a key challenge arises: *the model no longer receives explicit task labels for incoming inputs*. Consequently, it must autonomously determine which task-specific prompt pool to employ for generating accurate predictions.

To address this, HiDe-Prompt (Wang et al., 2024) introduces an additional MLP head \hat{g}_ψ , as a task predictor. This head leverages the pre-trained unprompted feature $f_\theta(\mathbf{x})$ to predict the task label. However, as discussed in Section 3, treating each task as a distinct class can be suboptimal because tasks are defined by their order of appearance rather than by meaningful semantic differences. In response, Le et al. (2025a) increase the predictor’s output dimension to match the number of encountered relations, then derives the task label from the relation it classifies. Despite this, it still relies on pre-trained knowledge and overlooks the potential task-identification capabilities of the experts with specialized knowledge \mathcal{P}_t .

In contrast, our approach leverages Cascade Voting (Zhou et al., 2024) to determine task identity. By discarding the MLP-based classifier head, Cascade Voting eliminates the need for explicit training for task prediction. Instead, it employs a voting strategy in which the specialized knowledge of experts in each prompt pool \mathcal{P}_t is used collaboratively to determine the task identity for a given instance.

Formally, for an instance \mathbf{x} of relation r , let $\mathbf{z}_r^i = f_{\theta, \mathcal{P}_i}(\mathbf{x}) \in \mathbb{R}^d$ be the representation obtained by passing \mathbf{x} through the pre-trained transformer combined with prompt pool \mathcal{P}_i . We assume during the t -th task, the class-conditional distribution of $\mathcal{D}_{r,t}^i = \{\mathbf{z}_r^i = f_{\theta, \mathcal{P}_i}(\mathbf{x}) | (\mathbf{x}, r) \in \mathcal{D}_t\}$ follows a multivariate Gaussian distribution $\mathcal{N}(\boldsymbol{\mu}_{r,t}^i, \boldsymbol{\Sigma}_t^i)$ for each prompt pool \mathcal{P}_i trained up to task t and for all relations $r \in \mathcal{R}_t$, where the covariance $\boldsymbol{\Sigma}_t^i$ is shared by all relations within the task. Based on this assumption, we use the maximum likelihood estimator to approximate the mean and covariance as follows:

$$\boldsymbol{\mu}_{r,t}^i = \frac{1}{|\mathcal{D}_{r,t}^i|} \sum_{\mathbf{z}_r^i \in \mathcal{D}_{r,t}^i} \mathbf{z}_r^i, \quad (20)$$

$$\boldsymbol{\Sigma}_t^i = \frac{1}{|\mathcal{D}_t|} \sum_{r \in \mathcal{R}_t} \sum_{\mathbf{z}_r^i \in \mathcal{D}_{r,t}^i} (\mathbf{z}_r^i - \boldsymbol{\mu}_{r,t}^i)(\mathbf{z}_r^i - \boldsymbol{\mu}_{r,t}^i)^\top, \quad (21)$$

While each relation–prompt pool pair maintains its own mean vector, a single covariance matrix is shared among all relations within the same task to capture the global variability at the task level.

Because continual relation extraction precludes access to data from previously encountered tasks, no distribution can be established for how prompt pool \mathcal{P}_i affects any earlier task j with $j < i$. To overcome it, we employ cascade voting to determine the appropriate prompts for relation classification during inference. This approach comprises two stages. First, each prompt pool, conceptualized as a specialized set of experts for a given task, independently assesses and votes on the suitability of its prompts. Subsequently, votes from all prompt pools are aggregated to identify the most appropriate prompt pool for the given instance.

Voting Procedure of a Prompt Pool. The voting procedure of a prompt pool \mathcal{P}_i begins by passing the input \mathbf{x} through the pre-trained backbone f_θ combined with the prompt pool \mathcal{P}_i to obtain the feature $\mathbf{z}^i = f_{\theta, \mathcal{P}_i}(\mathbf{x})$. Given that each relation $r \in \mathcal{R}_t$ is characterized by stored multivariate Gaussian distributions $\mathcal{N}(\boldsymbol{\mu}_{r,t}^i, \boldsymbol{\Sigma}_t^i)$, we compute the voting score of \mathcal{P}_i for each task $t \geq i$. In particular, we measure the Mahalanobis distance between \mathbf{z}^i and each Gaussian $\{\mathcal{N}(\boldsymbol{\mu}_{r,t}^i, \boldsymbol{\Sigma}_t^i) | r \in \mathcal{R}_t\}$, thereby producing \mathcal{P}_i ’s decision for task t as follows:

$$\text{Score}_t^i(\mathbf{x}) = \min_{r \in \mathcal{R}_t} (\mathbf{z}^i - \boldsymbol{\mu}_{r,t}^i)^\top \boldsymbol{\Sigma}_t^{i-1} (\mathbf{z}^i - \boldsymbol{\mu}_{r,t}^i), \quad t \geq i. \quad (22)$$

Finally, the outcome task identity predicted by \mathcal{P}_i is determined by:

$$\mathcal{V}^i(\mathbf{x}) = \arg \min_t \text{Score}_t^i(\mathbf{x}), \quad t \geq i. \quad (23)$$

Cascade Voting Mechanism. As the range of tasks covered by each prompt pool can vary, we adopt a cascade voting mechanism to mitigate boundary mismatches across prompt pools. We first employ the pre-trained BERT model \mathcal{P}_0 as the initial expert. Since both \mathcal{P}_0 and \mathcal{P}_1 can predict any subsequent task, their voting results are considered first. If \mathcal{P}_0 and \mathcal{P}_1 concur on a task label, that label is immediately assigned to \mathbf{x} .

If \mathcal{P}_0 and \mathcal{P}_1 disagree, we then gather votes from all relevant prompt pools $\{\mathcal{P}_i | i \in [\text{start}, \text{end}]\}$, where *start* and *end* derive from the ranges indicated by the disagreement between the two initial predictors. The task identity that receives the majority of votes is assigned to \mathbf{x} , and the corresponding prompt pool is selected for subsequent relation classification. This cascade voting strategy thus limits the number of prompt pools involved at each decision step and effectively handles inconsistencies in prediction ranges. A detailed algorithmic description is provided in Algorithm 1. Our approach enhances task-identity prediction accuracy, as demonstrated in Section 5.3, leading to improved TII performance and, consequently, more effective continual relation extraction, as described by Equation (1).

Comparison to MLP-based Approach. Both the MLP-based head strategy proposed by Le et al. (2025a) and the cascade voting mechanism introduced by Zhou et al. (2024) share the common principle of treating each observed relation independently, rather than grouping all relations within a single task into a unified category. In the MLP-based paradigm, each head corresponds to a specific relation, while in the cascade voting framework, every relation within a task is scored and a single highest-scoring relation is selected as that task’s representative. Subsequently, the representatives from all tasks are assessed together, and the task yielding the highest score is designated as the final classification decision.

A key distinction lies in *whether task classification is explicitly trained*. Under the MLP-based paradigm, a standard supervised task-prediction approach is employed: each task is allocated its own MLP head, and the classification result is given by the head returning the highest probability. In contrast, cascade voting dispenses with the MLP classifier, instead leveraging inference-time computations (e.g., distance-based metrics) to identify the most appropriate task.

Regarding memory usage, the MLP-based approach only requires storing relation-specific distributions to facilitate data reconstruction and mitigate catastrophic forgetting. The cascade voting mechanism, however, also relies on relation distributions that are further specialized by each prompt pool, resulting in a larger overall number of stored distributions compared to the MLP-based counterpart. Despite this increased memory demand, a notable advantage of cascade voting is that it *eliminates additional training overhead*, thereby expediting the overall training process compared to MLP-based classifiers.

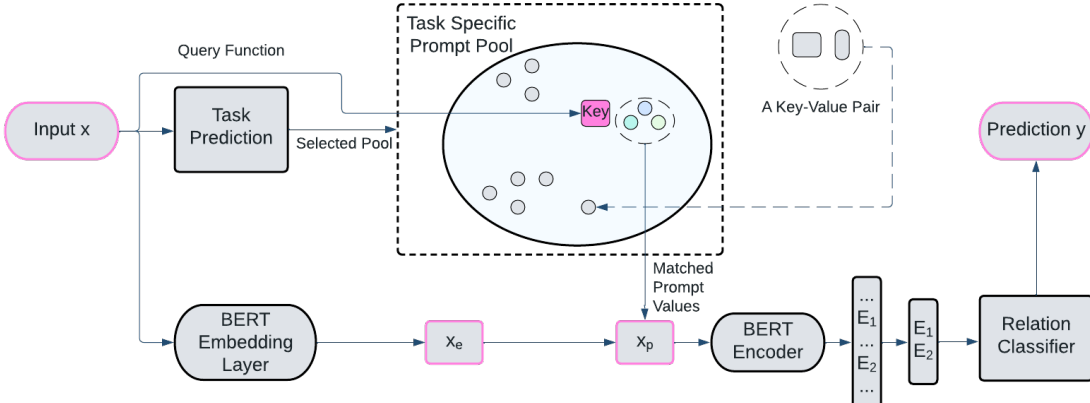


Figure 4: Data flow diagram. First, the task identity of the input \mathbf{x} is inferred via cascade voting, which determines the appropriate prompt pool. The input \mathbf{x} then queries this prompt pool to retrieve prompts whose keys most closely match the query $q(\mathbf{x})$. The selected prompt is prepended to the embedded input \mathbf{x}_e , yielding the prompted input \mathbf{x}_p . This prompted input is fed into the BERT encoder, from which the embeddings at the positions of the entities E_1 and E_2 are extracted and concatenated. Finally, this concatenated embedding is passed to the relation classifier g_ϕ , which predicts the relation label y of the original input \mathbf{x} .

4.4. Mitigating Classification Bias with Generative Models

A key element of our framework is the MLP head relation classifier g_ϕ . To mitigate catastrophic forgetting, we retain the representations of previously learned relations by deploying a generator that encodes their input distribution. Specifically, we employ Gaussian distributions $\mathcal{N}(\mu_r^t, \Sigma_r^t)$ for each relation $r \in \mathcal{R}_t$, where $\mu_r^t = \mu_{r,t}^t$ and $\Sigma_r^t = \Sigma_{r,t}^t$. These are computed from the prompt pool \mathcal{P}_t of the current task as described in Section 4.3.

By using a prompt-based generative model, the representations of previously learned relations can be reconstructed and replayed for subsequent tasks, thereby preserving essential relational knowledge. For each

Algorithm 2 \mathcal{T}_t training process

Input: Training t -th dataset \mathcal{D}_t , relation set \mathcal{R}_t
Output: Prompt pool \mathcal{P}_t and relation classifier ϕ

```
1: Randomly initialize  $\mathcal{P}_t$ 
2: for  $epoch \leftarrow 1$  to  $training\_epoch$  do
3:   for batch  $\mathbf{x}_B \subset \mathcal{D}_t$  do
4:     Update  $\mathcal{P}_t$  and  $g_\phi$  on  $\mathbf{x}_B$  via Equation (19)
5:   end for
6: end for
7: Update  $\hat{\mathcal{R}}_t \leftarrow \hat{\mathcal{R}}_{t-1} \cup \mathcal{R}_t$ 
8: for each  $r \in \mathcal{R}_t$  do
9:   for  $i \leftarrow 1$  to  $t$  do
10:    Compute  $\mu_{r,t}^i$  and  $\Sigma_t^i$  via Equation (20) and Equation (21)
11:   end for
12: end for
13: Train the relation classifier  $\phi$  via Equation (24)
14: return  $\mathcal{P}_t, \phi$ 
```

relation, storage requirements are minimal: only a mean vector and a covariance matrix are kept, significantly reducing memory overhead while preserving learned features. Furthermore, this design effectively addresses the issue of catastrophic forgetting by eliminating the need to store observed instances explicitly. Instead, the generative models capture and reproduce the distribution of the input space, enabling the model to simulate previously encountered relations without directly accessing historical data. This approach not only enhances computational efficiency but also ensures compliance with privacy constraints, as raw data is never retained.

These generative models produce a representation set \mathbf{z}_r for each relation r , which is then used to train the relation classifier. The MLP classifier g_ϕ is trained by minimizing the cross-entropy loss as below:

$$\mathcal{L}(\phi) = \sum_{i=1}^t \sum_{r \in \mathcal{R}_i} \sum_{\mathbf{z}_r \sim \mathcal{N}(\mu_r^i, \Sigma^i)} -\log \frac{\exp(g_\phi(\mathbf{z}_r)[r])}{\sum_{r' \in \hat{\mathcal{R}}_t} \exp(g_\phi(\mathbf{z}_r)[r'])}. \quad (24)$$

For a comprehensive overview of the training procedure, each phase is detailed in Algorithm 2. The data flow diagram illustrating the inference process is provided in Figure 4.

5. Experiments

5.1. Experimental Settings

Datasets. To ensure consistency and fairness in our evaluation, we follow the protocols outlined by Zhou et al. (2024); Le et al. (2025a) and assess the performance of WAVE++ on two widely used CRE datasets:

- **TACRED** (Zhang et al., 2017) comprises 106,264 instances spanning 41 relation types. instances spanning 41 relation types. Following the experimental setup of Cui et al. (2021), we partition this dataset into 10 distinct subsets.
- **FewRel** (Han et al., 2018) contains 56,000 instances encompassing 80 relation types. In accordance with Wang et al. (2019), we divide this dataset into 10 subsets.

Baseline Models. We compare WAVE++ with various prompt-based methods, including L2P (Wang et al., 2022b), HiDe-Prompt (Wang et al., 2024), EoE (Zhou et al., 2024) and WAVE-CRE (Le et al., 2025a). Notably, WAVE-CRE (Le et al., 2025a) is a simplified version of WAVE++. While WAVE-CRE also employs task-specific prompt pools, WAVE++ extends this strategy by integrating label descriptions to better capture relational information, as well as replacing MLP classifier with cascade voting for task identity prediction.

We further contrast our approach with traditional rehearsal-based methods: RP-CRE (Cui et al., 2021), ACA (Wang et al., 2022b), CRL (Zhao et al., 2022), CDec (Xia et al., 2023), CEAR (Zhao et al., 2023), RationaleCL (Xiong et al., 2023), CREST (Le et al., 2024c), and DP-CRE (Huang et al., 2024). For all methods, we utilize a pre-trained BERT encoder (Devlin, 2018) as the backbone architecture. We report model performance in terms of average accuracy across five distinct random runs.

FewRel										
Model	\mathcal{T}_1	\mathcal{T}_2	\mathcal{T}_3	\mathcal{T}_4	\mathcal{T}_5	\mathcal{T}_6	\mathcal{T}_7	\mathcal{T}_8	\mathcal{T}_9	\mathcal{T}_{10}
RP-CRE	97.9	92.7	91.6	89.2	88.4	86.8	85.1	84.1	82.2	81.5
ACA	98.3	95.0	92.6	91.3	90.4	89.2	87.6	87.0	86.3	84.7
CRL	98.1	94.6	92.5	90.5	89.4	87.9	86.9	85.6	84.5	83.1
CDec	98.4	95.4	93.2	92.1	91.0	89.7	88.3	87.4	86.4	84.8
CEAR	98.1	<u>95.8</u>	93.6	91.9	91.1	89.4	88.1	86.9	85.6	84.2
RationaleCL	98.6	95.7	93.4	<u>92.3</u>	<u>91.3</u>	89.7	88.2	87.3	86.3	<u>85.1</u>
CREST	<u>98.7</u>	93.6	<u>93.8</u>	<u>92.3</u>	91.0	<u>89.9</u>	87.6	86.7	86.0	84.8
DP-CRE	98.5	95.4	93.7	92.1	90.9	89.4	<u>88.5</u>	<u>87.4</u>	86.3	<u>85.1</u>
L2P	97.4	90.8	83.6	76.5	68.9	64.1	61.0	57.4	50.1	44.6
HiDe-Prompt	95.5	89.4	86.0	85.7	87.8	84.2	75.9	75.1	70.3	67.2
EoE	97.8	95.0	93.6	92.5	91.6	90.0	88.9	87.9	86.9	85.5
WAVE-CRE	97.9	95.5	93.6	92.4	91.1	90.2	88.7	87.6	86.5	85.0
WAVE++	98.2	95.8	95.1	94.1	92.7	91.9	90.2	89.9	89.0	87.7
TACRED										
Model	\mathcal{T}_1	\mathcal{T}_2	\mathcal{T}_3	\mathcal{T}_4	\mathcal{T}_5	\mathcal{T}_6	\mathcal{T}_7	\mathcal{T}_8	\mathcal{T}_9	\mathcal{T}_{10}
RP-CRE	97.6	90.6	86.1	82.4	79.8	77.2	75.1	73.7	72.4	72.4
ACA	98.0	92.1	90.6	85.5	84.4	82.2	80.0	78.6	78.8	78.1
CRL	97.7	93.2	89.8	84.7	84.1	81.3	80.2	79.1	79.0	78.0
CDec	97.7	92.8	91.0	86.7	85.2	82.9	80.8	80.2	78.8	78.6
CEAR	97.7	94.3	<u>92.3</u>	<u>88.4</u>	<u>86.6</u>	84.5	82.2	81.1	80.1	79.1
RationaleCL	<u>98.6</u>	<u>94.4</u>	91.5	88.1	86.5	<u>84.9</u>	<u>84.5</u>	<u>82.5</u>	<u>81.6</u>	<u>80.8</u>
CREST	97.3	91.4	82.3	82.5	79.2	75.8	78.8	77.4	78.6	79.4
DP-CRE	97.8	93.8	91.5	87.5	85.7	84.2	82.9	81.3	81.5	80.7
L2P	96.9	88.2	73.8	68.6	66.3	63.1	60.4	59.1	56.8	54.8
HiDe-Prompt	97.3	92.8	86.2	82.6	80.6	80.4	75.8	73.7	72.9	72.6
EoE	98.7	94.7	90.6	87.8	87.2	85.9	84.3	83.2	82.7	81.5
WAVE-CRE	98.4	94.3	91.6	87.8	85.7	83.5	81.3	80.4	79.5	78.7
WAVE++	97.6	93.6	90.7	88.2	86.4	85.4	84.3	83.7	83.2	82.5

Table 2: Average accuracy (%) of all methods across learning stages for FewRel and TACRED dataset. The best accuracy scores under the rehearsal-free and rehearsal-based setting are in **bold** and underlined, respectively.

Implementation Details. All experiments were conducted on a single NVIDIA A100 GPU. We employed random search to tune the hyperparameters of WAVE++, while the baseline methods used the configurations reported by Zhao et al. (2022), allowing for fair comparisons. Specifically, we froze the parameters of the pre-trained BERT model and optimized only the MLP-based relation classifiers and the prompt pools. Under these conditions, training WAVE++ took approximately seven hours on the FewRel dataset and one hour on the TACRED dataset.

5.2. Main Results

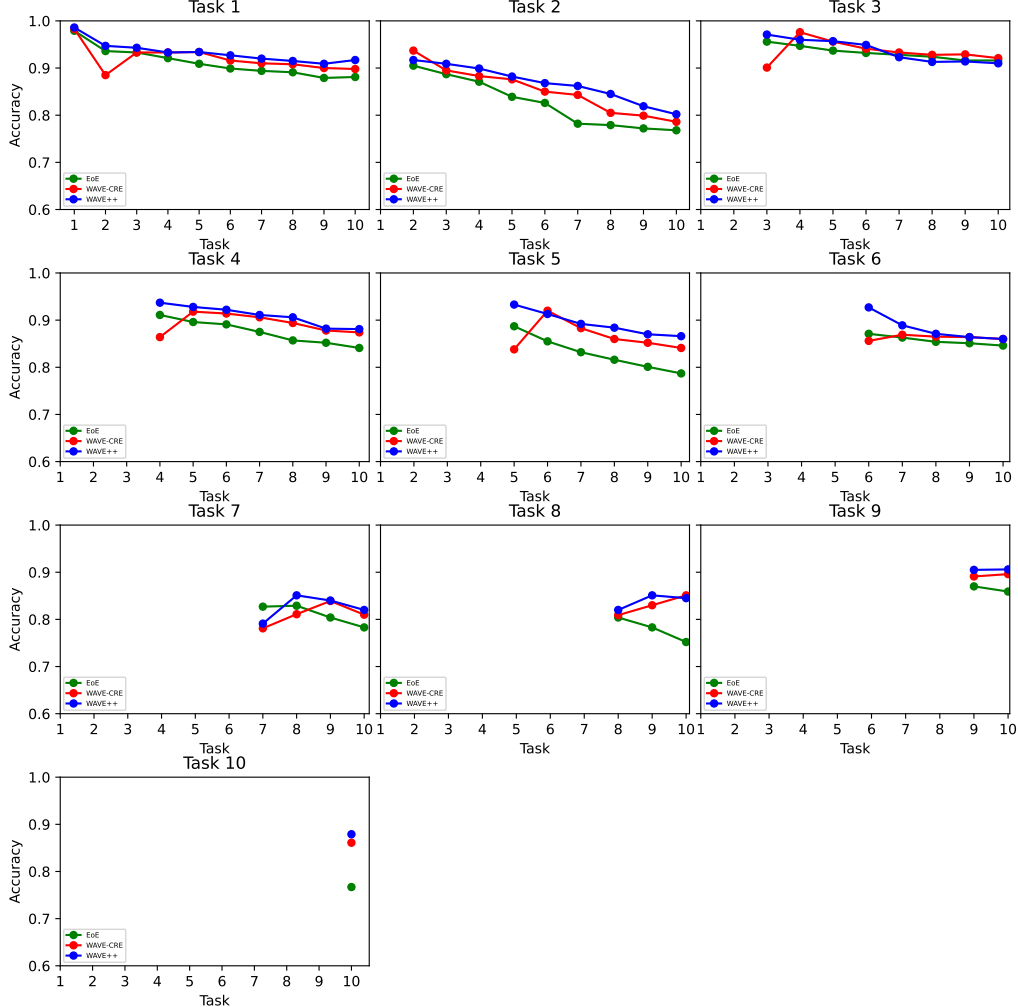


Figure 5: Variation in average accuracy (%) for individual tasks during the training process using WAVE++, WAVE-CRE, and EoE on the FewRel dataset.

In Table 2, we present a detailed performance comparison of WAVE++ against both rehearsal-free and rehearsal-based CRE methods. We first benchmarked WAVE++ against other rehearsal-free approaches,

finding that it consistently outperforms all baselines. Notably, on the FewRel dataset at the final task, WAVE++ exceeds the performance of the second-best method, EoE, by 2%. Furthermore, WAVE++ surpasses all other methods across various stages of training, as demonstrated in Figure 5, where the accuracy of WAVE++ progressively outperforms EoE during training. Although WAVE++ shows minor dips relative to EoE at certain points on TACRED, its performance on the final tasks, as well as in scenarios with an increasing number of tasks, ultimately reflects its superior resistance to catastrophic forgetting.

In addition, WAVE++ demonstrates substantial improvements over its predecessor, WAVE-CRE, throughout the training process. By the final task, WAVE++ achieves an accuracy that surpasses WAVE-CRE by approximately 2% on FewRel and 4% on TACRED. The accuracy across individual tasks also shows significant improvement over the course of training, as depicted in Figure 5. These gains can largely be attributed to the incorporation of label descriptions and an enhanced voting-based task prediction mechanism, as opposed to the previous MLP-based approach. Further details on these improvements will be discussed in Section 5.3.

Furthermore, we evaluate WAVE++ against recent state-of-the-art, rehearsal-based CRE methods. Despite not utilizing a memory buffer for replay, WAVE++ outperforms all evaluated rehearsal-based methods. On both datasets, WAVE++ demonstrates a significant performance advantage and exhibits robust resistance to catastrophic forgetting, even in the absence of prior sample storage. These findings underscore the effectiveness and efficiency of WAVE++ as a robust solution for continual relation extraction.

5.3. Ablation Studies

FewRel										
Model	\mathcal{T}_1	\mathcal{T}_2	\mathcal{T}_3	\mathcal{T}_4	\mathcal{T}_5	\mathcal{T}_6	\mathcal{T}_7	\mathcal{T}_8	\mathcal{T}_9	\mathcal{T}_{10}
WAVE++ w/o Prompt Pool	96.1	93.9	92.6	92.4	90.3	89.4	88.5	87.9	87.9	86.4
WAVE++	98.2	95.8	95.1	94.1	92.7	91.9	90.2	89.9	89.0	87.7
TACRED										
Model	\mathcal{T}_1	\mathcal{T}_2	\mathcal{T}_3	\mathcal{T}_4	\mathcal{T}_5	\mathcal{T}_6	\mathcal{T}_7	\mathcal{T}_8	\mathcal{T}_9	\mathcal{T}_{10}
WAVE++ w/o Prompt Pool	97.5	92.8	89.1	85.9	84.4	83.7	83.1	81.9	81.6	81.1
WAVE++	97.6	93.6	90.7	88.2	86.4	85.4	84.3	83.7	83.2	82.5

Table 3: Average accuracy (%) of WAVE++ with and without prompt pool. The best result for each dataset and metric is **bolded**.

Task-Specific Prompt Pool. To assess the impact of the task-specific prompt pool on the performance of WAVE++, we conducted experiments under two conditions: WAVE++ with a prompt pool and WAVE++ with only a single task-specific prompt per task. The detailed results are presented in Table 3. The inclusion of a prompt pool enhances performance across both datasets. As discussed in Section 4.1, the prompt pool enables the dynamic selection of prefix experts within each task, rather than relying on a fixed set. This flexibility allows the model to better capture task-specific variations, leading to improved performance.

Label Descriptions. To comprehensively evaluate the impact of label descriptions, we conducted experiments comparing EoE and our proposed WAVE++ model under two conditions: one with label descriptions and one without. As presented in Table 4, the removal of label descriptions results in a reduction of approximately 2% in the average accuracy of WAVE++ across both datasets. The inclusion of label descriptions provides additional contextual information, thereby facilitating more effective and robust learning of relational features, which in turn enhances classification performance. These findings emphasize the important role of label descriptions in capturing essential relational characteristics and improving within-task predictions.

FewRel										
Model	\mathcal{T}_1	\mathcal{T}_2	\mathcal{T}_3	\mathcal{T}_4	\mathcal{T}_5	\mathcal{T}_6	\mathcal{T}_7	\mathcal{T}_8	\mathcal{T}_9	\mathcal{T}_{10}
WAVE++ w/o Description	96.9	94.0	92.6	91.7	90.9	89.8	88.7	88.2	87.2	85.8
WAVE++	98.2	95.8	95.1	94.1	92.7	91.9	90.2	89.9	89.0	87.7
TACRED										
Model	\mathcal{T}_1	\mathcal{T}_2	\mathcal{T}_3	\mathcal{T}_4	\mathcal{T}_5	\mathcal{T}_6	\mathcal{T}_7	\mathcal{T}_8	\mathcal{T}_9	\mathcal{T}_{10}
WAVE++ w/o descriptions	97.4	93.0	89.1	86.0	84.4	83.5	82.8	81.8	81.1	80.7
WAVE++	97.6	93.6	90.7	88.2	86.4	85.4	84.3	83.7	83.2	82.5

Table 4: Average accuracy (%) of WAVE++ with and without label descriptions. The best result for each dataset and metric is **bolded**

TACRED										
Model	\mathcal{T}_1	\mathcal{T}_2	\mathcal{T}_3	\mathcal{T}_4	\mathcal{T}_5	\mathcal{T}_6	\mathcal{T}_7	\mathcal{T}_8	\mathcal{T}_9	\mathcal{T}_{10}
EoE	98.7	94.7	90.6	87.8	87.2	85.9	84.3	83.2	82.7	81.5
EoE + descriptions	98.8	95.3	91.3	88.0	87.5	86.1	84.8	83.6	83.0	81.9

Table 5: Average accuracy (%) of EoE with and without label descriptions. The best result for each dataset and metric is **bolded**

Additionally, label descriptions significantly improve the accuracy of EoE on the TACRED dataset, as shown in Table 5. This further demonstrates the effectiveness of label descriptions as a valuable component in enhancing continual relation extraction performance.

FewRel										
Num of descriptions	\mathcal{T}_1	\mathcal{T}_2	\mathcal{T}_3	\mathcal{T}_4	\mathcal{T}_5	\mathcal{T}_6	\mathcal{T}_7	\mathcal{T}_8	\mathcal{T}_9	\mathcal{T}_{10}
w/o descriptions	96.9	94.0	92.6	91.7	90.9	89.8	88.7	88.2	87.2	85.8
1 description	98.2	95.8	95.1	94.1	92.7	91.9	90.2	89.9	89.0	87.7
3 descriptions	97.7	<u>95.3</u>	<u>94.1</u>	<u>93.2</u>	92.3	<u>91.4</u>	<u>90.2</u>	89.6	88.8	87.4
5 descriptions	97.7	<u>95.3</u>	94.0	93.1	92.3	91.4	90.3	89.7	88.8	87.5
7 descriptions	97.8	<u>95.3</u>	<u>94.1</u>	<u>93.1</u>	<u>92.3</u>	91.3	90.3	<u>89.8</u>	<u>88.9</u>	87.6
TACRED										
Num of descriptions	\mathcal{T}_1	\mathcal{T}_2	\mathcal{T}_3	\mathcal{T}_4	\mathcal{T}_5	\mathcal{T}_6	\mathcal{T}_7	\mathcal{T}_8	\mathcal{T}_9	\mathcal{T}_{10}
w/o descriptions	97.4	93.0	89.1	86.0	84.4	83.5	82.8	81.8	81.1	80.7
1 description	<u>97.6</u>	93.6	<u>90.7</u>	88.2	<u>86.4</u>	85.4	84.3	83.7	83.2	82.5
3 descriptions	97.5	94.0	90.8	88.8	<u>86.4</u>	84.8	84.1	82.9	<u>82.6</u>	81.9
5 descriptions	97.3	<u>93.9</u>	<u>90.7</u>	87.7	86.3	84.4	83.9	<u>83.2</u>	82.6	<u>82.1</u>
7 descriptions	97.7	93.4	90.3	<u>88.5</u>	86.8	<u>85.2</u>	<u>84.2</u>	83.1	82.5	82.1

Table 6: Detailed analyses of WAVE++ with different number of descriptions. For each dataset and metric, the best result is **bolded** and the second is underlined.

Number of Label Descriptions D . To explore the impact of the number of label descriptions D in Equation (18) on the performance of WAVE++, we conducted experiments using the FewRel and TACRED datasets with varying values of D . Specifically, we tested configurations with D ranging from zero to seven. The results, presented in Table 6, demonstrate that WAVE++ maintains consistent performance even with a limited number of label descriptions. These findings indicate that WAVE++ is not heavily reliant on a large number

of label descriptions for effective performance. In fact, the model achieves high accuracy with only a few descriptions, thus offering a favorable balance between predictive capability and computational efficiency. This characteristic highlights the versatility of WAVE++ for practical scenarios, where acquiring extensive label descriptions may be challenging or costly.

Settings	TACRED									
	\mathcal{T}_1	\mathcal{T}_2	\mathcal{T}_3	\mathcal{T}_4	\mathcal{T}_5	\mathcal{T}_6	\mathcal{T}_7	\mathcal{T}_8	\mathcal{T}_9	\mathcal{T}_{10}
$L=8, K=1$	97.3	93.3	90.2	87.9	86.0	84.9	84.1	83.2	82.7	82.3
$L=4, K=2$	97.3	93.4	90.3	88.0	86.2	85.1	84.2	83.3	82.8	82.2
$L=2, K=4$	97.5	93.4	90.5	88.1	86.2	85.2	84.0	83.5	82.7	82.1
$L=1, K=8$	97.6	93.6	90.7	88.2	86.4	85.4	84.3	83.7	83.2	82.5

Table 7: Detailed analyses of the number of experts L within a prompt. The best result is **bolded**.

Number of Experts per Prompt L . Similarly, we investigate the impact of varying the prompt length L on model performance. The number of prompts selected, K , was adjusted to maintain a consistent total number of experts across experiments, ensuring a fair comparison. The results are summarized in Table 7. As discussed in Section 4.1, setting $L = 1$ provides greater flexibility in expert selection, thereby enhancing the model’s expressiveness, since each prefix expert is assigned a distinct key within the prompt pool. Empirical results demonstrate that setting $L = 1$ yields the best performance compared to other values of L .

Model	FewRel									
	\mathcal{T}_1	\mathcal{T}_2	\mathcal{T}_3	\mathcal{T}_4	\mathcal{T}_5	\mathcal{T}_6	\mathcal{T}_7	\mathcal{T}_8	\mathcal{T}_9	\mathcal{T}_{10}
EoE	100	95.3	95.7	94.4	92.5	91.6	88.3	87.5	86.8	86.0
WAVE-CRE	100	96.8	94.5	93.3	91.0	89.5	88.6	87.6	86.4	85.4
WAVE++	100	97.9	96.1	95.1	94.0	92.7	91.7	90.8	89.6	88.3

Model	TACRED									
	\mathcal{T}_1	\mathcal{T}_2	\mathcal{T}_3	\mathcal{T}_4	\mathcal{T}_5	\mathcal{T}_6	\mathcal{T}_7	\mathcal{T}_8	\mathcal{T}_9	\mathcal{T}_{10}
EoE	100	95.2	87.5	85.0	82.0	82.4	83.3	82.7	84.1	82.4
WAVE-CRE	100	96.8	91.1	86.8	84.9	83.6	82.1	80.4	80.2	79.2
WAVE++	100	95.9	92.0	90.5	88.7	87.9	86.9	85.9	85.2	84.8

Table 8: Task prediction accuracy (%) of WAVE-CRE and WAVE++. The best result for each dataset and metric is **bolded**.

Task Identity Inference. Instead of employing a conventional MLP head for task classification, we utilize a cascade voting mechanism for task identity prediction. This approach not only reduces training overhead but also enhances task identification by aggregating predictions from all prompt pools during the selection process. To assess its effectiveness relative to an MLP-based method, such as WAVE-CRE (Le et al., 2025a), we conducted a controlled experiment measuring task classification accuracy, with results presented in Table 8.

The results demonstrate that WAVE++ significantly outperforms WAVE-CRE, with an approximate improvement of 3% on the FewRel dataset and 4% on TACRED after training on all tasks. In addition to these gains in raw accuracy, the cascade voting mechanism exhibits greater stability compared to the MLP-based classifier. In particular, the MLP-based approach shows occasional sharp declines in accuracy, indicative of its sensitivity to distribution shifts when new tasks are introduced. In contrast, the voting mechanism maintains consistent performance, highlighting its robustness in managing heterogeneous task distributions. Moreover,

WAVE++ surpasses EoE in terms of task prediction accuracy. These findings underscore the effectiveness and resilience of the cascade voting mechanism in complex, multi-task scenarios, where adaptability and robustness to distribution shifts are crucial.

6. Conclusion

In this paper, we introduce a novel perspective on prompt-based continual learning by interpreting existing methods through the lens of mixture of experts models. We show that contemporary prompt-based continual learning approaches can be viewed as a special case of MoE architectures. Building on this insight, we present WAVE++, which shares key conceptual similarities with sparse MoE designs. Our framework addresses several challenges in prompt-based continual learning, including suboptimal task identification, sensitivity to distribution shifts, and handling within-task diversity. Specifically, we mitigate these issues by employing a cascade voting mechanism for task prediction and using task-specific prompt pools, complemented by label descriptions to enhance continual relation extraction performance.

Despite these advancements, there remain hurdles to improving the efficiency and effectiveness of WAVE++. Notably, the method heavily depends on the design of prompt pools and experts, suggesting opportunities to refine and optimize these components. While our approach attenuates catastrophic forgetting, retaining knowledge of previous tasks remains challenging, echoing issues highlighted in prior studies. In particular, if prompt pools are not properly applied during testing, model forgetfulness may reemerge. Moreover, although prompt pools enhance the expressiveness of our method, the current prefix-tuning experts are relatively simplistic. Future work may explore more sophisticated expert architectures to further strengthen the model.

References

Borchert, P., De Weerdt, J., Moens, M.F., 2024. Efficient information extraction in few-shot relation classification through contrastive representation learning. arXiv preprint arXiv:2403.16543 .

Caccia, L., Aljundi, R., Asadi, N., Tuytelaars, T., Pineau, J., Belilovsky, E., 2021. New insights on reducing abrupt representation change in online continual learning. arXiv preprint arXiv:2104.05025 .

Cui, L., Yang, D., Yu, J., Hu, C., Cheng, J., Yi, J., Xiao, Y., 2021. Refining sample embeddings with relation prototypes to enhance continual relation extraction, in: Proceedings of the 59th Annual Meeting of the Association for Computational Linguistics and the 11th International Joint Conference on Natural Language Processing (Volume 1: Long Papers), pp. 232–243.

Dao, V., Pham, V.C., Tran, Q., Le, T.T., Ngo, L., Nguyen, T., 2024. Lifelong event detection via optimal transport, in: Proceedings of the 2024 Conference on Empirical Methods in Natural Language Processing, pp. 12610–12621.

Devlin, J., 2018. Bert: Pre-training of deep bidirectional transformers for language understanding. arXiv preprint arXiv:1810.04805 .

Du, N., Huang, Y., Dai, A.M., Tong, S., Lepikhin, D., Xu, Y., Krikun, M., Zhou, Y., Yu, A.W., Firat, O., et al., 2022. Glam: Efficient scaling of language models with mixture-of-experts, in: International Conference on Machine Learning, PMLR. pp. 5547–5569.

Hai, N.L., Nguyen, T., Van, L.N., Nguyen, T.H., Than, K., 2024. Continual variational dropout: a view of auxiliary local variables in continual learning. Machine Learning 113, 281–323.

Han, X., Dai, Y., Gao, T., Lin, Y., Liu, Z., Li, P., Sun, M., Zhou, J., 2020. Continual relation learning via episodic memory activation and reconsolidation, in: Proceedings of the 58th Annual Meeting of the Association for Computational Linguistics, pp. 6429–6440.

Han, X., Zhu, H., Yu, P., Wang, Z., Yao, Y., Liu, Z., Sun, M., 2018. Fewrel: A large-scale supervised few-shot relation classification dataset with state-of-the-art evaluation. arXiv preprint arXiv:1810.10147 .

Houlsby, N., Giurgiu, A., Jastrzebski, S., Morrone, B., De Laroussilhe, Q., Gesmundo, A., Attariyan, M., Gelly, S., 2019. Parameter-efficient transfer learning for nlp, in: International conference on machine learning, PMLR. pp. 2790–2799.

Hu, E.J., Shen, Y., Wallis, P., Allen-Zhu, Z., Li, Y., Wang, S., Wang, L., Chen, W., 2021. Lora: Low-rank adaptation of large language models. arXiv preprint arXiv:2106.09685 .

Huang, M., Xiao, M., Wang, L., Du, Y., 2024. DP-CRE: Continual relation extraction via decoupled contrastive learning and memory structure preservation, in: Calzolari, N., Kan, M.Y., Hoste, V., Lenci, A., Sakti, S., Xue, N. (Eds.), Proceedings of the 2024 Joint International Conference on Computational Linguistics, Language Resources and Evaluation (LREC-COLING 2024), ELRA and ICCL, Torino, Italia. pp. 5338–5349. URL: <https://aclanthology.org/2024.lrec-main.475/>.

Jacobs, R.A., Jordan, M.I., Nowlan, S.J., Hinton, G.E., 1991. Adaptive mixtures of local experts. Neural Computation 3.

Ji, B., Yu, J., Li, S., Ma, J., Wu, Q., Tan, Y., Liu, H., 2020. Span-based joint entity and relation extraction with attention-based span-specific and contextual semantic representations, in: Proceedings of the 28th international conference on computational linguistics, pp. 88–99.

Jordan, M.I., Jacobs, R.A., 1994. Hierarchical mixtures of experts and the em algorithm. *Neural computation* 6, 181–214.

Ke, Z., Liu, B., 2022. Continual learning of natural language processing tasks: A survey. *arXiv preprint arXiv:2211.12701* .

Kim, G., Xiao, C., Konishi, T., Ke, Z., Liu, B., 2022. A theoretical study on solving continual learning. *Advances in neural information processing systems* 35, 5065–5079.

Le, M., Luu, T.N., The, A.N., Le, T.T., Nguyen, T., Nguyen, T.T., Van, L.N., Nguyen, T.H., 2025a. Adaptive prompting for continual relation extraction: A within-task variance perspective, in: Proceedings of the AAAI Conference on Artificial Intelligence.

Le, M., Nguyen, A., Nguyen, H., Nguyen, C., Ho, N., 2025b. Adaptive prompt: Unlocking the power of visual prompt tuning. *arXiv preprint arXiv:2501.18936* .

Le, M., Nguyen, A., Nguyen, H., Nguyen, T., Pham, T., Van Ngo, L., Ho, N., 2024a. Mixture of experts meets prompt-based continual learning. *Advances in Neural Information Processing Systems* 38.

Le, M., Nguyen, C., Nguyen, H., Tran, Q., Le, T., Ho, N., 2025c. Revisiting prefix-tuning: Statistical benefits of reparameterization among prompts, in: The Thirteenth International Conference on Learning Representations.

Le, T.T., Dao, V., Nguyen, L., Nguyen, T.N., Ngo, L., Nguyen, T., 2024b. Sharpseq: Empowering continual event detection through sharpness-aware sequential-task learning, in: Proceedings of the 2024 Conference of the North American Chapter of the Association for Computational Linguistics: Human Language Technologies (Volume 1: Long Papers), pp. 3632–3644.

Le, T.T., Nguyen, M., Nguyen, T.T., Van, L.N., Nguyen, T.H., 2024c. Continual relation extraction via sequential multi-task learning, in: Proceedings of the AAAI Conference on Artificial Intelligence, pp. 18444–18452.

Lester, B., Al-Rfou, R., Constant, N., 2021. The power of scale for parameter-efficient prompt tuning. *arXiv preprint arXiv:2104.08691* .

Li, J., Wang, X., Zhu, S., Kuo, C.W., Xu, L., Chen, F., Jain, J., Shi, H., Wen, L., 2024. Cumo: Scaling multimodal lilm with co-upcycled mixture-of-experts. *arXiv preprint arXiv:2405.05949* .

Li, X.L., Liang, P., 2021. Prefix-tuning: Optimizing continuous prompts for generation. *arXiv preprint arXiv:2101.00190* .

Liu, Y., Hu, J., Wan, X., Chang, T.H., 2022. A simple yet effective relation information guided approach for few-shot relation extraction. *arXiv preprint arXiv:2205.09536* .

Luo, D., Gan, Y., Hou, R., Lin, R., Liu, Q., Cai, Y., Gao, W., 2024. Synergistic anchored contrastive pre-training for few-shot relation extraction, in: Proceedings of the AAAI Conference on Artificial Intelligence, pp. 18742–18750.

Ma, J., Zhao, Z., Yi, X., Chen, J., Hong, L., Chi, E.H., 2018. Modeling task relationships in multi-task learning with multi-gate mixture-of-experts, in: Proceedings of the 24th ACM SIGKDD international conference on knowledge discovery & data mining, pp. 1930–1939.

McCloskey, M., Cohen, N.J., 1989. Catastrophic interference in connectionist networks: The sequential learning problem, in: Psychology of learning and motivation. Elsevier. volume 24, pp. 109–165.

Nguyen, C.V., Achille, A., Lam, M., Hassner, T., Mahadevan, V., Soatto, S., 2019. Toward understanding catastrophic forgetting in continual learning. arXiv preprint arXiv:1908.01091 .

Nguyen, H., Nguyen, C., Ngo, L., Luu, A., Nguyen, T., 2023. A spectral viewpoint on continual relation extraction, in: Findings of the Association for Computational Linguistics: EMNLP 2023, pp. 9621–9629.

Petrov, A., Torr, P.H., Bibi, A., 2023. When do prompting and prefix-tuning work? a theory of capabilities and limitations. arXiv preprint arXiv:2310.19698 .

Phan, H., Tuan, A.P., Nguyen, S., Linh, N.V., Than, K., 2022. Reducing catastrophic forgetting in neural networks via gaussian mixture approximation, in: Pacific-Asia Conference on Knowledge Discovery and Data Mining, Springer. pp. 106–117.

Riquelme, C., Puigcerver, J., Mustafa, B., Neumann, M., Jenatton, R., Susano Pinto, A., Keysers, D., Houlsby, N., 2021. Scaling vision with sparse mixture of experts. Advances in Neural Information Processing Systems 34, 8583–8595.

Shazeer, N., Mirhoseini, A., Maziarz, K., Davis, A., Le, Q., Hinton, G., Dean, J., 2017. Outrageously large neural networks: The sparsely-gated mixture-of-experts layer. arXiv preprint arXiv:1701.06538 .

Team, G., Anil, R., Borgeaud, S., Alayrac, J.B., Yu, J., Soricut, R., Schalkwyk, J., Dai, A.M., Hauth, A., Millican, K., et al., 2023. Gemini: a family of highly capable multimodal models. arXiv preprint arXiv:2312.11805 .

Team, G., Georgiev, P., Lei, V.I., Burnell, R., Bai, L., Gulati, A., Tanzer, G., Vincent, D., Pan, Z., Wang, S., et al., 2024. Gemini 1.5: Unlocking multimodal understanding across millions of tokens of context. arXiv preprint arXiv:2403.05530 .

Thanh, N.X., Le, A.D., Tran, Q., Le, T.T., Van, L.N., Nguyen, T.H., 2025. Few-shot, no problem: Descriptive continual relation extraction .

Tran, Q., Le, M., Truong, T., Phung, D., Ngo, L., Nguyen, T., Ho, N., Le, T., 2024a. Leveraging hierarchical taxonomies in prompt-based continual learning. arXiv preprint arXiv:2410.04327 .

Tran, Q., Thanh, N., Anh, N., Hai, N., Le, T., Ngo, L., Nguyen, T., 2024b. Preserving generalization of language models in few-shot continual relation extraction, in: Proceedings of the 2024 Conference on Empirical Methods in Natural Language Processing, pp. 13771–13784.

Van, L.N., Hai, N.L., Pham, H., Than, K., 2022. Auxiliary local variables for improving regularization/prior approach in continual learning, in: Pacific-Asia conference on knowledge discovery and data mining, Springer. pp. 16–28.

Vaswani, A., 2017. Attention is all you need. Advances in Neural Information Processing Systems .

Wang, H., Xiong, W., Yu, M., Guo, X., Chang, S., Wang, W.Y., 2019. Sentence embedding alignment for lifelong relation extraction. arXiv preprint arXiv:1903.02588 .

Wang, L., Xie, J., Zhang, X., Huang, M., Su, H., Zhu, J., 2024. Hierarchical decomposition of prompt-based continual learning: Rethinking obscured sub-optimality. Advances in Neural Information Processing Systems 36.

Wang, Y., Ma, Z., Huang, Z., Wang, Y., Su, Z., Hong, X., 2023a. Isolation and impartial aggregation: A paradigm of incremental learning without interference, in: Proceedings of the AAAI Conference on Artificial Intelligence, pp. 10209–10217.

Wang, Z., Liu, Y., Ji, T., Wang, X., Wu, Y., Jiang, C., Chao, Y., Han, Z., Wang, L., Shao, X., et al., 2023b. Rehearsal-free continual language learning via efficient parameter isolation, in: Proceedings of the 61st Annual Meeting of the Association for Computational Linguistics (Volume 1: Long Papers), pp. 10933–10946.

Wang, Z., Zhang, Z., Ebrahimi, S., Sun, R., Zhang, H., Lee, C.Y., Ren, X., Su, G., Perot, V., Dy, J., et al., 2022a. Dualprompt: Complementary prompting for rehearsal-free continual learning, in: European Conference on Computer Vision, Springer. pp. 631–648.

Wang, Z., Zhang, Z., Lee, C.Y., Zhang, H., Sun, R., Ren, X., Su, G., Perot, V., Dy, J., Pfister, T., 2022b. Learning to prompt for continual learning, in: Proceedings of the IEEE/CVF conference on computer vision and pattern recognition, pp. 139–149.

Xia, H., Wang, P., Liu, T., Lin, B., Cao, Y., Sui, Z., 2023. Enhancing continual relation extraction via classifier decomposition. arXiv preprint arXiv:2305.04636 .

Xiong, W., Song, Y., Wang, P., Li, S., 2023. Rationale-enhanced language models are better continual relation learners. arXiv preprint arXiv:2310.06547 .

Yang, K., Zheng, N., Dai, X., He, L., Huang, S., Chen, J., 2020. Enhance prototypical network with text descriptions for few-shot relation classification, in: Proceedings of the 29th ACM International Conference on Information & Knowledge Management, pp. 2273–2276.

Zhang, Y., Zhong, V., Chen, D., Angeli, G., Manning, C.D., 2017. Position-aware attention and supervised data improve slot filling, in: Conference on empirical methods in natural language processing.

Zhao, K., Xu, H., Yang, J., Gao, K., 2022. Consistent representation learning for continual relation extraction. arXiv preprint arXiv:2203.02721 .

Zhao, W., Cui, Y., Hu, W., 2023. Improving continual relation extraction by distinguishing analogous semantics. arXiv preprint arXiv:2305.06620 .

Zhou, S., Li, Y., Miao, X., Qian, T., 2024. An ensemble-of-experts framework for rehearsal-free continual relation extraction, in: Findings of the Association for Computational Linguistics ACL 2024, pp. 1410–1423.

Zhou, Y., Du, N., Huang, Y., Peng, D., Lan, C., Huang, D., Shakeri, S., So, D., Dai, A.M., Lu, Y., et al., 2023. Brainformers: Trading simplicity for efficiency, in: International Conference on Machine Learning, PMLR. pp. 42531–42542.